INTERNATIONAL JOURNAL OF SCIENCE AND NATURE

www.scienceandnature.org

CORROSION INHIBITION OF CARBON STEEL BY NEW PHENYL QUINAZOLINONE DERIVATIVE IN 1M HCl: EXPERIMENTAL AND THEORETICAL INVESTIGATION

Rehab Majed Kubba, Ahmad Shalaan Alag & Suaad M. H. Al-Majidi
Department of Chemistry, College of Science, University of Baghdad, Baghdad, Iraq.

ABSTRACT
Newly synthesized quinazolinone derivative namely 2-[(3-phenyl-4-oxo-3,4-dihydroquinazolinone-2-yl-thio) aceto] phenyl thiosemicarbazide (PQPS) was investigated experimentally as a corrosion inhibitor for carbon steel in 1M HCl at various concentrations and different temperature using potentiodynamic polarization, and Scanning Electron Microscopy (SEM) measurements. The thermodynamic parameters obtained supported a physical adsorption mechanism and the adsorption followed Langmuir adsorption isotherm. Polarization curves showed that the compound acts as a mixed inhibitor. A maximum inhibition efficiency of 96.75% has been achieved using (5ppm) of inhibitor. SEM image confirmed that the presence of the inhibitor forms a protective film on the surface of the carbon steel decreasing the corrosion process. Theoretically, quantum mechanics calculations of the approximate semi empirical method PM3 and Density Functional Theory (DFT) of (B3LYP) with a level of 6-311G ++ (2p, 2d) by using Gaussian-09 program were done to evaluate the structural, electronic and reactivity parameters of (PQPS) in relation to their effectiveness as a corrosion inhibitor in vacuum and two liquid media (DMSO and H_2O).

KEYWORDS: Corrosion inhibitor, PQPS, 1M HCl solution.

INTRODUCTION

Corrosion is the deterioration of metal by chemical attack or reaction with its environment. It is a constant and continuous problem, often difficult to eliminate completely (Rani and Basu, 2012). Carbon steel corrosion has been a problem of enormous practical importance due to its high cost on the national economy. Mild steel is an important material which finds wide applications in the industry due to its excellent mechanical properties. It is extensively used in various industries as a construction material for chemical reactors, heat exchanger and boiler systems, storage tanks, and oil and gas transport pipelines (Singh and Quraishi, 2012). An aqueous solution of acids is among the most corrosive media. Hydrochloric acid is the most difficult of the common acids to handle from the standpoints of corrosion and materials of constructions. Extreme care is required in the selection of materials to handle the acid by itself, even in relatively dilute concentrations or in process solutions containing an appreciable amount of hydrochloric acid. This acid is very corrosive to most of the common metals and alloys (Fontana, 1987). Preventing the corrosion of carbon steel has played an important role in various industries. Acids are widely used in industrial processes, such as pickling, cleaning, descaling. Thus the use of corrosion inhibitors is one of the most practical methods for corrosion protection of steel especially in acidic media (Bentiss *et al*., 2000). Most of the well-known corrosion inhibitors are organic compounds that mainly contain oxygen, sulfur, and nitrogen atoms and multiple bonds in the molecule through which they are adsorbed onto metal surfaces (Saxena *et al*., 2009, Raja and Sethuraman, 2008). Quinazolinone is a heterocyclic chemical compound with two conjoined aromatic rings incorporating with two nitrogen atoms, and one of the carbons oxidized with keto oxygen. Chemically it is known as Quinazolin-4(3*H*)-one (Chen *et al*., 2006). There are two structural isomers for quinazolinone, 2-quinazolinone (A) and 4-quinazolinone (B), with the 4-isomer being the more common Figure 1.

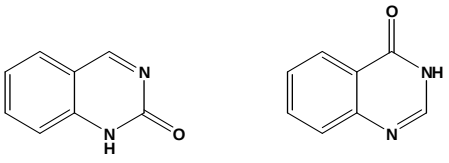

Quinazolin-2 (1H)-one (A) Quinazolin-4 (3H)-one (B)

FIGURE 1: The isomer structures of quinazolinone

The inhibitory activity of these molecules is accompanied by their adsorption to the metal surface. Free electron pairs on heteroatoms or π electrons are readily available for sharing to form a bond and act as nucleophile centers for inhibitor molecules and greatly facilitate the adsorption process over the metal surface, whose atoms act as

electrophiles. Recently, the effectiveness of an inhibitor molecule has been related to it's spatial as well as electronic structure (Ebenso *et al*., 2010). Quantum chemical methods are ideal tools for investigating these parameters and are able to provide insight into the inhibitor–surface interaction. The molecular structure and the electronic parameters that can be obtained through theoretical calculations, such as the Highest Occupied Molecular Orbital (HOMO) energy, the Lowest Unoccupied Molecular Orbital (LUMO) energy, the energy gap ($\Delta E=E_{LUMO}-E_{HOMO}$), are involved in the activity of the inhibitors (Obot and Obi-Egbedi, 2008). The inhibition performance is evaluated by polarization curves. Several isotherms are tested for their relevance to describe the adsorption behavior of the compound studied.

MATERIALS & METHODS

Synthesis of inhibitor (PQPS)

(a). Synthesis of 2-mercpto-3-phenyl-4(3H) quinazolin one (Alafeefy, 2011)

A mixture of 8.228g (0.06mol) anthranilic acid, 7.22ml (0.06mol) of phenylisothiocyanate and 6ml of triethylamine in 100ml absolute ethanol was refluxed for 3hours. The reaction mixture was cooled to room temperature, poured into ice-cold water, stirred and filtered. The precipitate was recrystallized from ethanol to give crystals.

(b). Synthesis of S-(α-Chloroaceto-2-yl)-3-phenyl-4(3H) quinazolinone (Al-Majidi, 2013)

To a mixture of 3g (0.01mol) compound (a) in 16ml of dimethylformamide (DMF), 0.662g (0.01mol) of anhydrous potassium hydroxide dissolve in (9ml) of methanol and (1ml, 0.01mol) chloroacetyl chloride added slowly. The mixture was refluxed for 4hours. Leaved stirring overnight, then poured into an ice water for precipitation, filtered and recrystallized from ethanol to give white crystals.

(c). Synthesis of 2-[(3-phenyl-4-oxo-3,4-dihydroquina zolin-2-yl) thio] acetohydrazide (Al-Majidi *et al*., 2013)

To a solution of compound (b) (4g, 0.012mol) in DMF (30ml), hydrazine hydrate 80% (2ml, 0.024mol) was added with continuous stirring in the round bottomed flask and the resulting mixture was refluxed for 4hours. After cooling the mixture, white precipitate was formed. The precipitate was filtered and recrystallized from ethanol.

(d). Synthesis of 2-[(3-phenyl-4-oxo-3,4dihydroquinazo linone-2-yl-thio) aceto] phenyl thiosemicarbazide (PQPS) (Al-Majidi and Al-Kaisy, 2009)

To a solution of compound (c) (2g, 0.006mol) in absolute ethanol (25ml), phenyl isothiocyanate (0.006mol, 0.81g) was added. Refluxed the mixture for 5hours, cooled, filtered and recrystallized from ethanol.

Preparation of test solutions

The blank solution of 1M HCl was prepared from (34.4%, 1.18g/ml) HCl by dilution with distilled water. The concentrations range of inhibitor was (5–30) ppm and the volume of test solution used for electrochemical measurement was 1L.

Methods of study

a. Computational

Calculations based on two sets of programs, the first set up is a software of MOPAC 2000 (Kandemirli and Sagdinc, 2007) with method calculation, and other is Gaussian software package 2009 and used approximate quasi-experimental with PM3 and density functional theory with B3LYP style with basis set 6-311G (2p, 2d,++) (Geerlings and Proft, 2002).

b. Electrochemical

An electrochemical cell containing three electrodes immersed in a solution, a carbon steel as a working electrode in the form of the disk was fitted into a polymer (bakelite) holder exposing 0.785cm^2 surface area to the solution, a platinum auxiliary electrode, and a silver-silver chloride (Ag/ AgCl, 3M KCl) reference electrode. The polarization curves were performed using a scan rate of 5mV.s^{-1} in the potential range of ±200mV around the open circuit potential (Eocp) using a Potentiostat/ Galvanostat. Measurements were performed in the 1M HCl solution without and containing different concentrations of the tested inhibitor. The temperature of solutions was held at 20, 30, 40, 50C by a thermostat water bath.

c. Microscopic

The carbon steel specimens used for surface morphology examination were immersed in 1M HCl without and with 5ppm of PQPS by using Scanning Electron Microscopy, the energy of the acceleration beam employed was 20kV and the scale bar for the images is 100μm.

RESULTS & DISCUSSION

Synthesis of the compounds

(a). 2-mercpto-3-phenyl-4(3H) quinazolinone

Compound (a) was prepared via intermolecular cyclization reaction of equimolar amounts of anthranilic acid and phenylisothiocyanate in present of triethylamine as a catalyst in ethanol. The mechanism is shown in Scheme 1 (Joule and Mills, 2010). Compound (a) was afforded with a yield of 89% and a melting point of 297 to 299^{o}C.

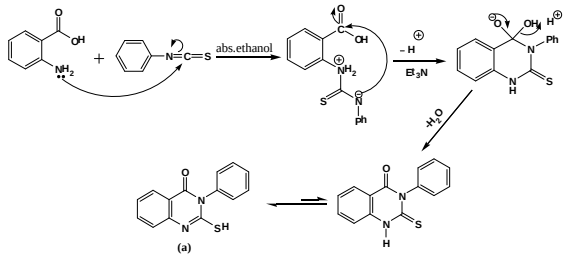

SCHEME1: The proposed mechanism for the compound **(a)** preparation reaction.

(b). Preparation of S-(α-Chloroaceto-2-yl)-3-phenyl-4(3H) quinazolinone.

Compound (b) was prepared by the nucleophilic substitution reaction of the compound (a) with Chlor-acetyl chloride. This reaction is carried out in alcoholic potassium hydroxide solution to increase the nucleophilicity of sulfur atom in attacking molecule by forming potassium salt as an intermediate. Compound (b) was afforded as a white solid with a yield of 96% and m.p of 158-160^{o}C. Also, silver nitrate alcoholic test confirmed the presence of chlorine group (Shriner et al., 1980). The mechanism of the reaction is shown in Scheme 2 (March, 1985).

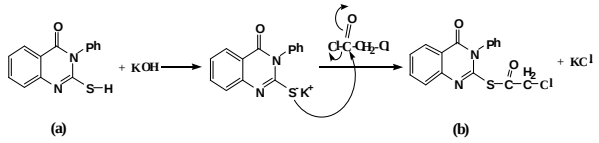

SCHEME 2: The proposed reaction mechanism for compound (**b**) preparation

(c). 2-[(3-phenyl-4-oxo-3,4-dihydro quinazolin-2-yl) thio] Aceto hydrazide

When compound (b) was refluxed with hydrazine hydrate in dimethylformamide as a solvent it gave the expected hydrazide derivative (c), Scheme 3. Compound (c) was afforded as a white solid with a yield of 60% and m.p of 260 to 262^{o}C.

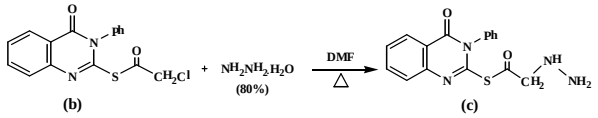

SCHEME 3: The proposed reaction mechanism for compound (**c**) preparation

(d). 2-[(3-phenyl-4-oxo-3,4-dihydro quinazolinone-2-yl-thio) aceto] phenyl thiosemicarbazide (PQPS)

The hydrazide derivative (c) was converted to compounds (d) via reaction with phenyl isothiocyanate in absolute ethanol Mechanism of the reaction involves nucleophilic attack of an amino group in compound (c) on deficient carbon in phenyl isothiocyanate followed by rearrangement (Ahmed, 2012) to form the PQPS compound, Scheme 4. PQPS was afforded as an off-white solid with a yield of 75% and m.p of 264 to 266^{o}C.

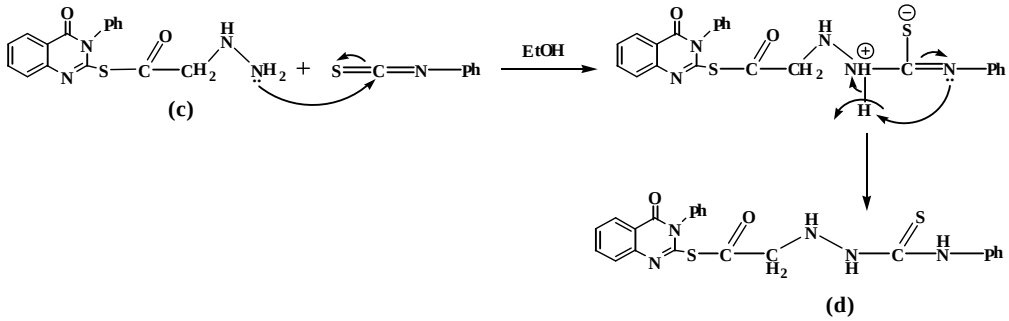

SCHEME 4: The proposed reaction mechanism for PQPS preparation

TABLE1: FTIR absorption bands and HNMR signals for PQPS compound

FTIR spectral data cm^{-1}					
ν(N-H)	ν(C-H) aromatic	ν(C-H) aliph.	ν(C=O)	ν(C=C) aromatic	Others
3355	3083	Sym. 2925 Assym. 2858	1715 Thio-ester 1691 Amide	1552 1512	1299 ν(C=S) 1620 ν(C=N)

^{1}HNMR signals δ (ppm)

3.35 (d, 2H, CH_2); 4.69 (d, 1H, CH_2-NH); 7.06 (s, 1H, oxazole ring); 7.42-8.49 (m, Ar-H); 9.54 (d, 1H, NH, oxazole ring).

Theoretical study

PM3 semiempirical method and DFT utilizing Becke three-parameter and the connection useful of Lee, Yang and Parr (B3LYP) together with the standard double-zeta plus polarization 6-311G++ (2p, 2d) [Parr and Yang, 1989, Becke, 1993, Lee et al., 1988), were carried out for figuring the optimize geometry of the investigate molecule in vacuum and two liquid media (DMSO and H_2O), implemented in the Gaussian 09 program package (Frisch et al., 2009).

Geometrical optimization structure

The final geometry of PQPS is given in Figure 2b. The optimization structural parameters such as bond angles,

bond distances and dihedral angles of the studied inhibitor are shown in Table 2. From Table 2, it is reflected that the longest bond length was observed for the S12-C13 bond ($1.812A^0$) due to the large bulky size of atom S comparing to others. The compound under investigation is not planar, possessing C_1 symmetry, Figure 2b. This result is confirmed by the values of bonds, bond angles, cis and trans dihedral angles, Table 2.

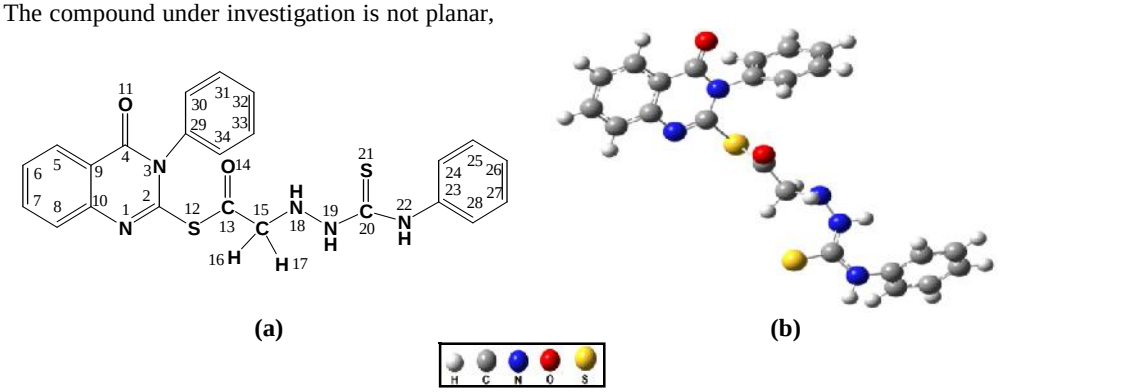

FIGURE 2: (a). Chemical structure of PQPS**, (b).** Equilibrium geometry of the PQPS molecule calculated by DFT **(**B3LYP/6311G++ (2p,2d)) method

TABLE 2: Calculated geometrical structure for PQPS molecule by using DFT method

Description Bond length	Bond length (Å)	Description angle (deg)	Angle (deg)	Description Dihedral angle (deg)	Dihedral angle (deg)
N1-C2	1.280G	N1C2N3	125.326	N1C2N3C4	1.232
N1-C10	1.384G	N1C2S12	116.664	N1C2N3C29	-178.712
C2-N3	1.383G	N1C10C8	118.787	N1C2S12C13	-91.068
C2-S12	1.802G	N1C10C9	121.844	N1C10C8H	0.021
N3-C4	1.422G	C2N1C10	118.267	N1C10C8C7	179.850
N3-C29	1.447G	C2N3C4	120.907	N1C10C9C4	0.431
C4-C9	1.463G	C2N3C29	122.585	N1C10C9C5	179.870
C4=O11	1.214G	C2S12C13	99.574	C2N1C10C8	-179.837
C5-H	1.080G	N3C2S12	117.977	C2N1C10C9	0.147
C5-C6	1.381G	N3C4C9	114.053	C2N3C4C9	-0.547
C5-C9	1.399G	N3C4O11	120.697	C2N3C4O11	179.676
C6-H	1.080G	N3C29C30	119.390	C2N3C29C30	91.395
C6-C7	1.402G	N3C29C34	119.662	C2S12C13O14	-10.807
C7-H	1.081G	C4N3C29	116.507	C2S12C13C15	167.889
C7-C8	1.380G	C4C9C5	120.175	C4N3C2S12	179.157
C8-H	1.080G	C4C9C10	119.590	C4N3C29C34	89.175
C8-C10	1.403G	C5C6H	120.049	C4C9C5H	-0.352
C9-C10	1.405G	C5C6C7	120.051	C4C9C5C6	179.699
S12-C13	1.812G	C5C9C10	120.233	C5C9C4O11	-0.140
C13=O14	1.199G	C6C5H	121.582	C5C9C10C8	0.113
C13-C15	1.514G	C6C5C9	119.838	C6C5C9C10	0.003
C15-H16	1.089G	C6C7H	119.685	C9C4N3C29	179.401
C15-H17	1.096G	C6C7C8	120.651	C10N1C2S12	-178.944
C15-N18	1.463G	C7C6H	119.899	C10C9C4O11	179.557
N18-H	1.016G	C7C8H	121.721	C10C9C5H	179.951
N18-N19	1.402G	C7C8C10	119.855	O11C4N3C29	-0.374
N19-H	1.006G	C8C7H	119.662	C10N1C2S12	-178.944
N19-C20	1.359G	C8C10C9	119.367	S12C2N3C29	-0.787
C20=S21	1.676G	C9C4O11	125.248	S12C13C15H16	34.017
C20-N22	1.364G	C9C5H	118.579	S12C13C15N18	154.433
N22-H	1.006G	C10C8H	118.422	C13C15N18H	54.842
N22-C23	1.428G	S12C13O14	124.132	C13C15N18N19	174.183
C23-C24	1.396G	S12C13C15	111.681	O14C13C15H16	-147.286
C23-C28	1.394G	C13C15H16	110.048	O14C13C15H17	95.467
C24-H	1.081G	C13C15H17	106.939	O14C13C15N18	-26.870
C24-C25	1.390G	C13C15N18	109.579	C15N18N19H	111.697
C25-H	1.081G	O14C13C15	124.172	C15N18N19C20	-88.053
C25-C26	1.391G	C15N18H	108.924	H16C15N18H	175.613
C26-H	1.080G	C15N18N19	111.688	H16C15N18N19	-65.045
C26-C27	1.391G	H16C15H17	108.151	H17C15N18H	-64.047
C27-H	1.080G	H16C15N18	109.463	H17C15N18N19	55.293
C27-C28	1.390G	H17C15N18	112.611	N18N19C20S21	8.690
C28-H	1.081G	N18N19H	113.982	N18N19C20N22	-171.626

C29-C30	1.389G	N18N19C20	123.674	HN18N19H	-128.480
C29-C34	1.387G	N19N18H	108.110	N19C20N22H	-174.606
C30-H	1.080G	N19C20S21	123.233	N19C20N22C23	3.809
C30-C31	1.389G	N19C20N22	115.637	C20N19N18H	31.767
C31-H	1.080G	C20N19H	119.357	C20N22C23C24	65.988
C31-C32	1.391G	C20N22H	113.643	C20N22C23C28	-115.949
C32-H	1.081G	C20N22C23	127.761	S21C20N19H	167.942
C32-C33	1.390G	S21C20N22	121.128	S21C20N22H	5.083
C33-H	1.080G	N22C23C24	120.594	S21C20N22C23	-176.499
C33-C34	1.390G	N22C23C28	119.604	N22C23C24C25	178.986
C34-H	1.079G	C23C24C25	119.965	N22C23C28C27	-177.926

Figure 3 shows the geometries optimization of compound studied in the vacuum including HOMO and LUMO density distributions. HOMO mainly located on thiosemicarbazide moiety, this would indicate that the preferred active sites for an electrophilic attack are located within the region around the nitrogen atoms. Moreover, the electronic density of LUMO is distributed at the aromatic rings of quinazolinone moiety.

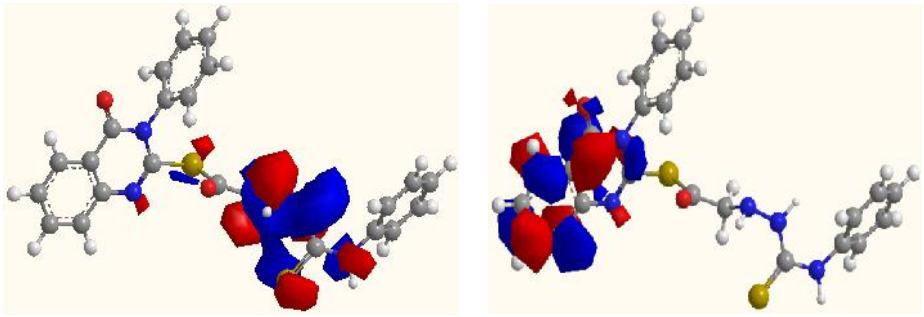

HOMO **LUMO**

FIGURE 3: DFT Frontier molecule orbital density distributions calculation for PQPS inhibitor. Red color: the negatively charged lobe, blue color: the positively charged lobe

Global molecular reactivity

The following quantum chemical indices were calculated: the energy of the highest occupied molecular orbital (E_{HOMO}), the energy of the lowest unoccupied molecular orbital (E_{LUMO}), energy gap (ΔE), dipole moment (μ), the number of transferred electrons (ΔN) were calculated by using the following equation (Khaled, 2008, Obot and Obi-Egbedi, 2010):

$$\Delta N = \frac{\chi_{Fe} - \chi_{inh.}}{[2(\eta_{Fe} + \eta_{inh.})]} \quad (1)$$

Where χ_{Fe} and $\chi_{inh.}$ denote the absolute electronegativity of carbon steel and the inhibitor molecule, respectively, η_{Fe} and η_{inh} denote the absolute hardness of carbon steel and the inhibitor molecule, respectively. χ_{Fe} and η_{Fe} values for carbon steel of 7.0eV mol^{-1} and 0.0eV mol^{-1}, respectively (Chermette, 1999). The electronegativity and hardness of the inhibitor are related to the Ionization potential IE and electron affinity EA, Equations 2-5.

$$\chi = \frac{IE+EA}{2} \quad (2)$$

$$\eta = \frac{IE-EA}{2} \quad (3)$$

$$IE = -E_{HOMO} \quad (4)$$

$$EA = -E_{LUMO} \quad (5)$$

Chemical Softness (S) and Global electrophilicity index (ω) were calculated according to the following equations respectively:

$$S = \frac{1}{\eta} \quad (6)$$

$$\omega = \frac{\chi^2}{2\eta} \quad (7)$$

The calculated parameters for the compound were presented in Table 3 according to the PM3 method and Table 4, Table 5 according to DFT method. Chemical reactivity of the molecules has been analyzed by these parameters. The HOMO energy (E_{HOMO}) is often associated with the electron donating ability of the molecule; therefore, inhibitors with high values of E_{HOMO} have a tendency to donate electrons to appropriate acceptor with low empty molecular orbital energy. Conversely, the LUMO energy (E_{LUMO}) indicates the electron-accepting ability of the molecule, the lowest its value the higher the capability of accepting electrons. The gap energy between the Frontier orbitals ($\Delta E_{HOMO-LUMO}$) is another important factor in describing the molecular activity, so when the gap energy decreased, the inhibitor efficiency is improved (Zhang *et al*., 2010). The dipole moment (μ in Debye) is a very important electronic parameter that results from the non-uniform distribution of charges on the various atoms in the molecule. The high value of dipole moment increases the adsorption between a chemical compound and metal surface (Wang *et al*., 2007). Chemical Hardness (η) measure of the ability of atom or molecule to transfer the charge and Chemical Softness (S) measure of the flexibility of an atom to receive electrons, compound possesses a high value of (η) and (S) is considered to be a good inhibitor. The ability of an atom or a group to pull electrons towards itself related to the electronegativity (χ), low electro negativity indicates

a good inhibitor. ω is the measure of the stability of an atom after gaining an electron, Low value of (ω) meaning the molecule has a good inhibition. The ΔN values are correlated to the inhibition efficiency resulting from electron donation. According to Lukovits et al. study (Lukovits *et al*., 2001), if ΔN<3.6, the inhibition efficiency increases with increasing electron- donating ability at the metal surface. The obtained values of ΔN reported in Table 3 according to PM3 and Table 5 according to DFT; show that all the calculated ΔN values are positive and lower than 3.6, indicates that the inhibitor molecules have the capability in donating electrons to the vacant d-orbital of metal.

TABLE 3: PM3 calculations of physical properties and quantum chemical parameters for PQPS inhibitor at the equilibrium geometry

ΔH^0_f kcal/mol	E_{HOMO} eV	E_{LUMO} eV	ΔE_{H-L} eV	μ Debye	IE eV	EA eV	¦= eV	¡ eV	S eV	[illegible]	ak
101.648	-8.997	-1.019	7.978	6.260	8.997	1.019	3.989	5.008	0.250	3.143	0.249

TABLE 4: DFT calculations for some physical properties of the PQPS molecule at the equilibrium geometry in the three media (vacuum, DMSO, and H_2O)

Inhibitor medium	Sym.	E_{HOMO} (eV)	E_{LUMO} (eV)	$\Delta E_{HOMO-LUMO}$ (eV)	μ (Debye)	E_{total} (eV)
Vacuum	C1	-6.079	-1.751	4.328	6.660	-57386.668
DMSO	C1	-6.463	-1.963	4.500	8.758	-57387.315
H_2O	C1	-6.471	-1.966	4.505	8.799	-57387.326

TABLE 5: Quantum chemical parameters for the PQPS molecule in the three media (vacuum, DMSO, and H_2O) as calculated using DFT method

Inhibitor medium	IE (eV)	EA (eV)	¦=(eV)	¡ (eV)	S (eV)	[illegible] (eV)	ak
Vacuum	6.079	1.751	2.164	3.915	0.462	3.541	0.712
DMSO	6.463	1.963	2.250	4.213	0.444	3.944	0.619
H_2O	6.471	1.966	2.252	4.218	0.444	3.950	0.617

Local reactivity for the 2-[(3-phenyl-4-oxo-3,4-dihydro quinazolinone-2-yl-thio) aceto] phenylthiosemicarb azide (POQS)

For the purpose of establishing the active sites of the inhibitor calculated molecules, three influencing factors: natural atomic charge, distribution of frontier molecular orbital and indices. According to the classical chemical theory, all chemical interactions are either by electrostatic or orbital interactions. The local reactivity of the studied inhibitor is investigated using the DFT Mulliken charges population analysis which means the receptive centers of particles (nucleophilic and electrophilic centers). Along these lines, the particle areas where the electronic charge is high are chemically milder than the locales where the electronic charge is little, so the electron density assumes an imperative part in ascertaining the compound reactivity. Chemical adsorption communications are taking place either by electrostatic or orbital collaborations. For effortlessness, just the charges on the nitrogen (N), oxygen (O), sulfur (S), ® -electrons of the quinazolinone ring which are donating electrons to carbon steel surface and some carbon particles are exhibited. Consequently, the favored destinations for nucleophilic reactive sites are N1, C6, O11, S12, O14, C15, N19, S21, C23, C26, C32 with the order of S21> S12> O11> C15> C6> C26> C32> O14> N19> C23> N1. For the most favored electrophilic reactive sites that can accept electrons are C2, C9 and C29 with the order of (C2> C9> C29) (which possess the highest positive charge on joining directly to the withdrawing aromatic ring) and (C4, C13, C20) atoms with the order of C13> C20> C4, which directly bonded to the oxygen and sulfur heteroatoms, Table 6. Consider the solvent effect, The values of the electronic charges for the nucleophilic and electrophilic reactive sites increase on going from vacuum to DMSO and H_2O solutions, making among adsorption by donating electron through sulfur atoms (S12, S21), the S atoms can donate and get the electron from the metal, because of possessing a lone pair of electrons and unfilled d orbital. The negative charge centers could offer electrons to the Fe atoms to form a coordinate bond. The positive charge centers can accept electrons from 3d orbital of the Fe atom to form feedback bond, thus further strengthening the interaction of inhibitor and Fe surface.

TABLE 6: DFT Mulliken charges population analysis for the calculated inhibitor molecule PQPS in three media (vacuum, DMSO and H_2O).

Atom	Electronic charge (ecu)	Atom	Electronic charge (ecu)	Atom	Electronic charge (ecu)
N1	**-0.153V**	**C13**	**0.469V**	**C25**	**-0.089V**
	-0.236D		**0.521D**		**-0.130D**
	-0.237w		**0.522w**		**-0.130w**
C2	**0.279V**	**O14**	**-0.277V**	**C26**	**-0.327V**
	0.383D		**-0.317D**		**-0.360D**
	0.385w		**-0.317w**		**-0.360w**
N3	**0.018V**	**C15**	**-0.400V**	**C27**	**-0.090V**

	0.064D		-0.420D		-0.116D
	0.065w		-0.420w		-0.117w
C4	0.121V	H16	0.132V	C28	-0.030V
	0.224D		0.156D		-0.020D
	0.226w		0.156w		-0.019w
C5	-0.041V	H17	0.094V	C29	0.333V
	-0.049D		0.097D		0.226D
	-0.049w		0.097w		0.224w
C6	-0.380V	N18	-0.034V	C30	-0.089V
	-0.432D		-0.079D		-0.089D
	-0.433w		-0.080w		-0.089w
C7	-0.110V	N19	-0.269V	C31	-0.165V
	-0.136D		-0.233D		-0.183D
	-0.136w		-0.232w		-0.183w
C8	0.001V	C20	0.351V	C32	-0.291V
	-0.013D		0.393D		-0.320D
	-0.013w		0.394w		-0.321w
C9	0.234V	S21	-0.686V	C33	-0.159V
	0.254D		-0.797D		-0.185D
	0.254w		-0.799w		-0.185w
C10	0.155V	N22	-0.023V	C34	-0.085V
	0.178D		-0.016D		-0.100D
	0.178w		-0.016w		-0.100w
O11	-0.435V	C23	-0.234V		
	-0.518D		-0.221D		
	-0.519w		-0.220w		
S12	-0.522V	C24	0.148V		
	-0.576D		0.130D		
	-0.577w		0.129w		

V: vacuum, D: dimethyl sulfoxide (DMSO), W: water, blue color: increase in electronic charge to more positive, red color: increase in electronic charge to more negative.

Corrosion measurement

Potentiostatic polarization measurements

The corrosion behavior can be determined by a polarization curve ($E_{corr.}$ vs log $I_{corr.}$). Using Tafel extrapolation method, it is possible to obtain the $I_{corr.}$ and the $E_{corr.}$ by the extrapolation of anodic and/or cathodic Tafel lines (Poorqasemi et al., 2009). The potentiodynamic polarization curves for carbon steel in 1M HCl at 293K in absence and presence different concentrations of PQPS are shown in Figure 4. The effect of increasing concentration and temperature on $E_{corr.}$, $I_{corr.}$, and Tafel slopes (bc and ba) are shown in Table 7, The protection efficiency was calculated from the following Equation:

$$\%PE = 1 - \frac{I}{I_0} \times 100 \qquad (8)$$

These results show that the compound (PQPS) acts as an effective inhibitor for corrosion of carbon steel in 1M HCl solution. The presence of PQPS in 1M HCl solution decrease corrosion current densities $I_{corr.}$ and shift corrosion potential $E_{corr.}$ to a more anodic and cathodic direction, suggesting PQPS can be described as a mixed-type inhibitor (anodic and/or cathodic) for corrosion of carbon steel in 1M HCl, showing its inhibitory action on both hydrogen evolution and metal dissolution. The protection efficiency decrease with increasing temperature suggesting the type of adsorption of the inhibitor on the sample surface is a physical adsorption (Maayta and Al-Rawashdeh, 2004, Abboud et al., 2009). Maximum protection efficiency for the compound (PQPS) was achieved at a concentration of 5ppm (1.084×10^{-5}M) and temperature of 293K. The corrosion rate C.R of carbon steel increases with increasing temperature both for inhibited and uninhibited solution. The C.R of carbon steel in 1M HCl solution decrease on adding the inhibitor to the solution.

I_o and I: the corrosion current densities in the absence and presence inhibitor, respectively.As well as surface coverage **Θ** and corrosion rate C.R which can be determined from the corrosion current densities ($I_{corr.}$).

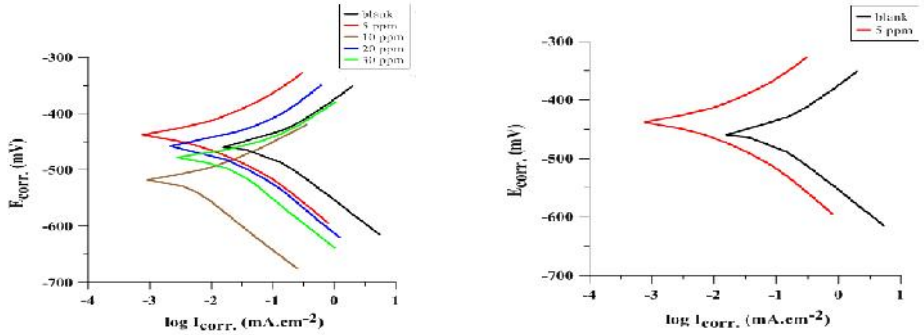

a **b**

FIGURE 4: Polarization plots of carbon steel in 1M HCl for blank and inhibitor at a temperature of 293K a. at various concentrations of PQPS. b. At the optimum concentration (5ppm) of PQPS.

TABLE 7: Electrochemical data of the carbon steel corrosion with 1M HCl at various concentrations of PQPS and different temperatures

Solun.	T (K)	Ecorr. (mV)	Icorr. (µA.cm-2)	Bc (mV.dec-1)	ba (mV.dec-1)	%PE	Ɵ	C.R mm.y-1
	293	-460.1	131.24	-120.3	102.1	.....	.....	1.521
Blank	303	-457.6	182.19	-106.8	77.3	.....	.....	2.111
1M HCl	313	-468.5	288.89	-132.7	94.2	.....	.....	3.348
	323	-441.1	528.72	-42.6	46.6	.....	……	6.128
	293	-437.9	4.26	-106.8	148.9	96.75	0.967	0.049
PQPS	303	-428.7	11.24	-186.2	188.9	93.83	0.938	0.130
5ppm	313	-470.7	30.72	-187.6	204.1	89.36	0.893	0.356
	323	-469.3	45.49	-125.0	72.1	91.39	0.913	0.527
	293	-518.7	4.52	-208.5	254.4	96.55	0.965	0.052
PQPS	303	-447.9	48.62	-59.0	41.8	73.31	0.733	0.563
10ppm	313	-436.9	45.77	--50.2	38.6	84.15	0.841	0.530
	323	-431.7	69.24	-35.9	33.5	86.90	0.869	0.802
	293	-458.3	18.51	-59.5	50.3	85.89	0.858	0.214
PQPS	303	-447.0	67.34	-74.0	44.6	63.03	0.630	0.780
20ppm	313	-425.0	40.13	-105.4	71.3	86.10	0.861	0.465
	323	-436.7	74.24	-112.2	90.4	85.95	0.859	0.860
	293	-478.8	20.12	-92.5	132.1	84.66	0.846	0.233
PQPS	303	-466.3	54.14	-71.9	51.9	70.28	0.702	0.627
30ppm	313	-457.7	65.31	-81.1	64.7	77.39	0.773	0.756
	323	-458.9	122.64	-90.2	83.9	76.80	0.768	1.421

Adsorption isotherm behavior

The adsorption characteristics of PQPS compound were analyzed to further establish the interaction mechanism between PQPS and the carbon steel (Abd El-Lateef et al., 2013, Gad and Tamous, 1990, Limousin et al., 2007). Adsorption of inhibitor involves the formation of two types of interaction responsible for bonding of inhibitor to a metal surface. The first one (physical adsorption) is weak undirected interaction and is due to electrostatic attraction between inhibiting organic ions or dipoles and the electrically charged surface of the metal. The second type of interaction (adsorption) occurs when directed forces govern the interaction between the adsorbate and adsorbent. Chemical adsorption involves charge sharing or charge transfer from adsorbates to the metal surface atoms in order to form a coordinate type of bond. Chemical adsorption has a free energy of adsorption and activation energy higher than physical adsorption and, hence, usually, it is irreversible (Trabanelli and Mansfeld, 1987). The adsorption behavior of PQPS was found to obey Langmuir isotherms. The Langmuir adsorption isotherm, given by Equation 9 (Li et al., 2012), showed the best fit for each data set.

$$\frac{C_{inh.}}{\Theta} = \frac{1}{K_{ads.}} + C_{inh.} \quad (9)$$

Where, $C_{inh.}$ is the inhibitor concentration (mol.L^{-1}), $K_{ads.}$ is the adsorption/desorption equilibrium constant (L.mol^{-1}).

The plot of $C_{inh.}/\Theta$ vs $C_{inh.}$ gave a straight line and the intercept represents ($1/K_{ads.}$) with a slight deviation of the slope from unity as shown in the correlation coefficient values, Figure 5.

The Gibbs free energy of adsorption ($\Delta G_{ads.}$) was calculated from Equation 10:

$$\Delta G_{ads.} = \Delta H_{ads.} - T\Delta S_{ads.} \quad (10)$$

Where $\Delta H_{ads.}$, $\Delta S_{ads.}$ are the change in enthalpy and entropy of adsorption respectively, calculated from plotting Log $K_{ads.}$ vs (1/ T), Equation 12.

$K_{ads.}$ is related to the standard Gibbs free energy of adsorption ($\Delta G_{ads.}$), Equation 11 (Shetty et al., 2007).

$$\Delta G_{ads.} = -2.303RT\,[\log 55.5K_{ads.}] \quad (11)$$

Where R is the universal gas constant 8.314 J.$mol.^{-1}.K^{-1}$, T is the temperature (K), and 55.5 is the molar concentration of water (mol. L^{-1}).

Equations 10 and 11 are combined to obtain Equation 12.

$$\text{Log } K_{ads.} = \frac{-\Delta H_{ads.}}{2.303RT} + \frac{\Delta S_{ads.}}{2.303R} + \text{Log } \frac{1}{55.5} \quad (12)$$

The enthalpy $\Delta H_{ads.}$ is obtained from the slope ($-\Delta H_{ads.}/2.303R$) obtained from plotting (log $K_{ads.}$) vs. (1/T). $\Delta S_{ads.}$ obtained from the intercept of [($\Delta S_{ads.}/2.303R$) +(log (1/ 55.5)] Figure 6.

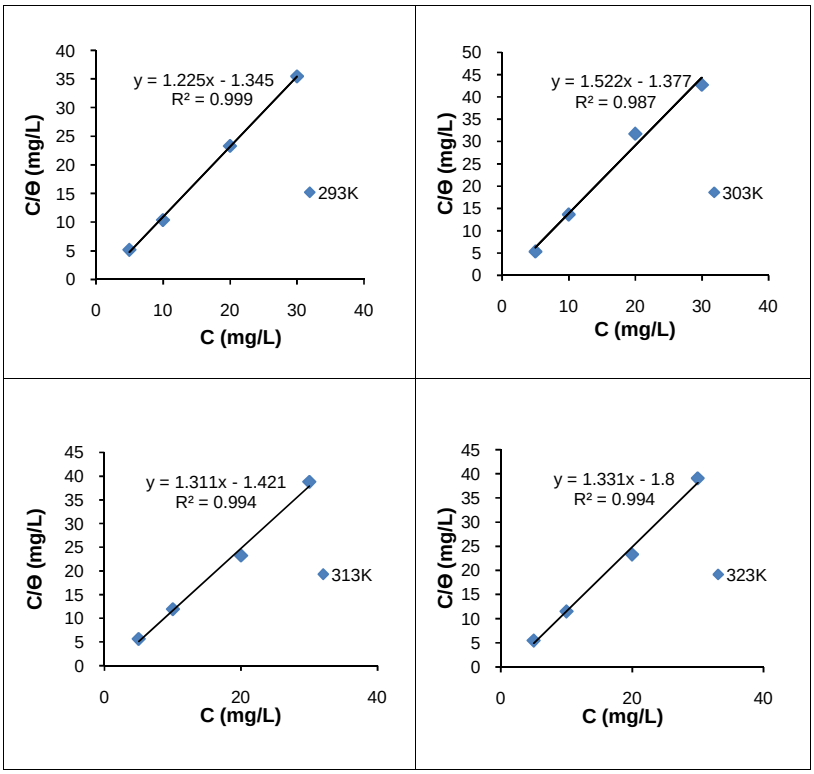

FIGURE 5: Langmuir isotherms plot for the adsorption of PQPS on carbon steel at the temperature range (293, 303, 313 and 323K).

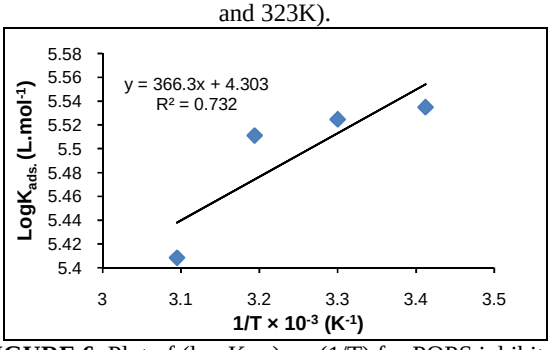

FIGURE 6: Plot of (log $K_{ads.}$) vs (1/T) for PQPS inhibitor.

TABLE 8: Langmuir adsorption parameters of PQPS with 1M HCl at different temperature and various concentrations.

T (K)	$K_{ads.}$ (L mol^{-1})	$\Delta G_{ads.}$ (kJ mol^{-1})	$\Delta H_{ads.}$ (kJ mol^{-1})	$\Delta S_{ads.}$ (kJ $mol^{-1}.K^{-1}$)	R^2
293	3.427×10^5	-40.94	-7.013	0.115	0.999
303	3.347×10^5	-42.10			0.987
313	3.244×10^5	-43.26			0.994
323	2.561×10^5	-44.41			0.994

The results show high values of $K_{ads.}$ indicate a strong interaction of PQPS with the carbon steel surface in 1M HCl (Safak *et al*., 2012). The negative values of $\Delta G_{ads.}$ ensure the spontaneity of the adsorption process and stability of the adsorbed layer on the carbon steel surface (Migahed, 2005). Generally, $\Delta G_{ads.}$ values (0 to -20 kJ/mol.) are associated with electrostatic interactions between the charged molecules and the charged metal surface (physisorption), whereas those below -40 kJ/mol. involve the sharing or transfer of charge from the organic molecules to the metal surface to form a coordinate covalent bond (chemisorption) (Bahrami *et al*., 2010, Behpour *et al*., 2010). The values range of $\Delta G_{ads.}$ was (-40.94 to -44.41) kJ.mol^{-1}, Table 8 refer to chemisorptions. Chemisorption of the molecular forms of PQPS could occur through donor/acceptor interactions between the ℞-electrons of the C=O group, C=S group, and the two aromatic rings, and the vacant d orbitals of the carbon steel surface atoms make it possible to provide electrons to the unoccupied d orbital of carbon steel surface to form stable coordination bonds (Khaled, 2008). The negative value of $\Delta H_{ads.}$ means the dissolution process is an exothermic phenomenon (Gomma and Wahdan, 1995). It assumed that an exothermic process is attributed to either physical or

chemical adsorption but endothermic process corresponds solely to chemisorption. In an exothermic process, physisorption is distinguished from chemisorption by considering the absolute value of a physisorption process is lower than 40 kJ.mol^{-1} while the adsorption heat of a chemisorption process approaches is a round 100 kJ.mol^{-1} (Zarrouk *et al*., 2010). The value of -7.013 kJ.mol^{-1} for ΔH_{ads}. postulates that a physisorption is more favored. ($\Delta S_{ads.}$) refers to random interaction, whenever it is less random the inhibitor is the best.

Corrosion kinetic and thermodynamic activation parameters

Activation parameters were calculated for blank and optimum concentration (5ppm) of PQPS. activation parameters at different temperatures (293, 303, 313, 323K) in the absence and presence of the 5ppm concentration of PQPS were calculated from Arrhenius and Arrhenius transition state equations (13,14) were used respectively (Dahmani *et al*., 2010, Singh *et al*., 2010).

$$\text{Log C.R} = \text{Log A} - \frac{Ea}{2.303\,RT} \quad (13)$$

$$\text{Log}\frac{C.R}{T} = \text{Log}\frac{R}{Nh} + \frac{\Delta S^*}{2.303R} - \frac{\Delta H^*}{2.303RT} \quad (14)$$

C.R is the corrosion rate (mm.y^{-1}), R is the universal gas constant (8.314 J.mol^{-1}.K^{-1}), T is temperature (K), A is the Arrhenius pre-exponential factor (cm^{-2}.s^{-1}), Ea is the activation energy (minimum amount of energy required to initiate a chemical adsorption) (kJ. mol^{-1}), h is the Plank's constant (6.626 x 10^{-34} J.s^{-1}), N is the Avogadro's number (6.022 x 10^{23} mol^{-1}), ΔS^* is the change in entropy of activation (kJ. mol^{-1}. K^{-1}) and ΔH^* is the change in enthalpy of activation (kJ. mol^{-1}).

The activation energy Ea and Arrhenius factor A, at the absence and presence of the optimum concentration (5 mg/L) of PQPS, was determined by linear regression between log C.R and 1/T, Figure 7.

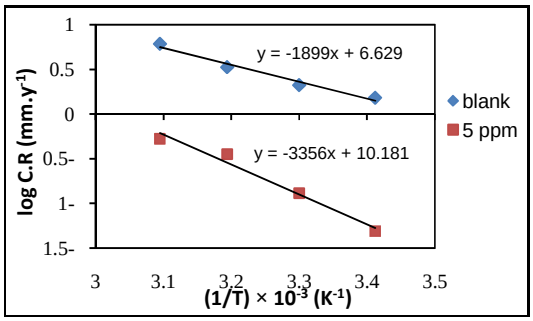

FIGURE 7: Plot of log C.R vs 1/T for the corrosion of carbon steel in 1M HCl at the optimum concentration (5 mg/L) of PQPS inhibitor within the blank

The enthalpy of activation ΔH^* is obtained from the slope (-ΔH^*/ 2.303R) obtained from plotting (log CR/T) vs. (1/T) with ΔS^* which obtained from an intercept of [(log (R/ Nh) + (ΔS^*/2.303R)], Figure 8.

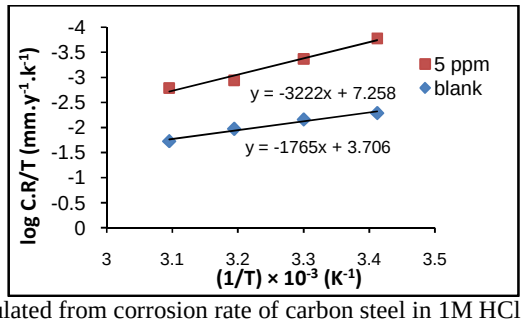

FIGURE 8: Arrhenius plots calculated from corrosion rate of carbon steel in 1M HCl in the absence and presence of the optimum concentration (5 mg/L) of PQPS.

The results showed that the value of Ea increase in the presence of PQPS suggesting inhibitor species being physically adsorbed on the carbon steel surface (Almeida et al., 1999, Bentiss et al., 2005, Mora et al., 2004) Table 9. The higher activation energy for inhibitors as compared to that of free acid may be explained according to Riggs and Hurd (Riggs and Hurd, 1967), as they stated that at higher levels of surface coverage the corrosion process may proceed on the adsorbed layer of inhibitor and not on the metal surface leading to a decrease in the apparent activation energy. The positive sign of enthalpies ΔH^* reflects the endothermic nature of dissolution process. The activation enthalpy ΔH^* increase in the presence of the inhibitor implies that the PQPS increase the height of the energy barrier of the corrosion process. The entropy of activation ΔS^* has negative value. The increase in the entropy (-0.127 to -0.059) kJ.mol^{-1}.K^{-1} from absence to the presence of PQPS reveals that an increase in disordering takes place in going from reactant to the activated complex. This behavior can be explained as a result of the replacement process of water molecules during adsorption of PQPS on carbon steel surface (Dahmani et al., 2010). The value of activation free energy explains that the corrosion reaction of carbon steel is non-spontaneous and

increase with increasing temperature, Table 9 suppose that corrosion reaction increase with increasing temperature.

TABLE 9: Activation parameters for the carbon steeldissolution in 1M HCl in the absence and presence the optimum

Solution	T (K)	ΔH^* (kJ.mol^{-1})	ΔG^* (kJ.mol^{-1})	ΔS^* (kJ.mol^{-1}.K^{-1})	Ea (kJ.mol^{-1})	A (Molecule.cm^{-2}. s^{-1})
Blank	293	33.795	70.889	-0.127	36.360	2.562×10^{30}
1M HCl	303		72.155			
	313		73.421			
	323		74.687			
PQPS	293	61.692	78.859	-0.059	64.258	9.114×10^{33}
5ppm	303		79.445			
	313		80.031			
	323		80.617			

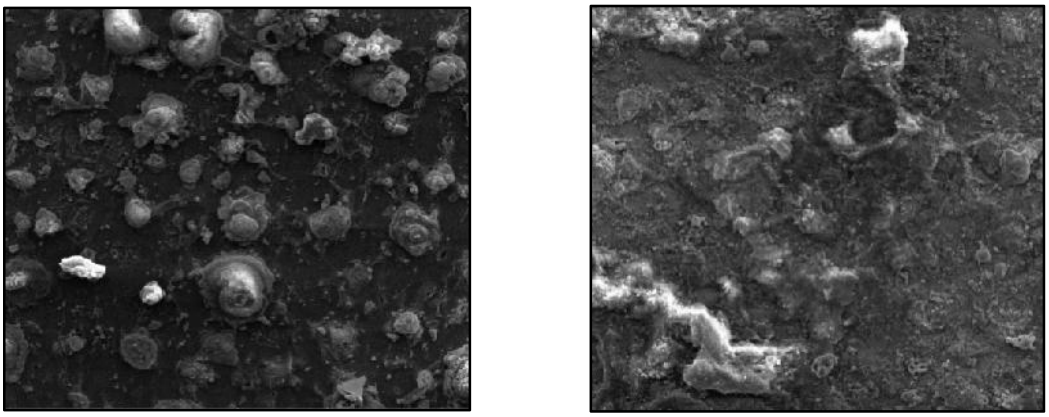

a **b**

FIGURE 9: SEM images for carbon steel surface with 1M HCl solution **a-** in the absence of PQPS, **b-** in the presence of (5ppm) PQPS.

concentration of the inhibitor

Explanation for adsorption of PQPS

It is a mixed complex type (comprehensive adsorption). This assumption is supported by the value of $\Delta G_{ads.}$, which is proposed by chemisorptions, and by the value of $\Delta H_{ads.}$, it is assumed that the physisorption is more favorable and the results obtained for the temperature dependence of the inhibition process, which decreases with the increase of temperature (physisorption) and the value of Ea suggesting that the inhibitor types are physically adsorbed on the surface of carbon steel, so the adsorption of PQPS on carbon steel surface in 1M HCl is supposed to be a complex in nature and predominantly physisorption.

Scanning Electron Microscopy (SEM)

Figure 9 present two SEM images recorded to investigate the changes occurred on the surface of the carbon steel in the absence and presence of inhibitor in 1M HCl solution. Figure 9a, shown the damaged of carbon steel surface in 1M HCl solution through forming a spherical particles due to an aggressive attack of the corroding medium. In presence of PQPS, the damage decreased, and a thin and uniform layer is observed Figure 9b. This may be interpreted due to the adsorption of PQPS and insulating the surface from the acidic medium, by forming a protective inhibitor film at the carbon steel surface.

CONCLUSION

- Theoretical calculations were done to evaluate the structural, electronic and reactivity parameters of (PQPS) in relation to their effectiveness as a corrosion inhibitor in vacuum and two liquid media (DMSO and H_2O).
- Geometrical studies found that PQPS is not a planer molecule, and the HOMO is mainly located on thiosemicarbazide moiety, this would indicate that the preferred active sites for an electrophilic attack are located within the region around the nitrogen atoms.
- Consider the solvent effect, the values of the electronic charges for the nucleophilic and electrophilic reactive sites increase on going from vacuum to DMSO and H_2O solutions.
- PQPS quinazolinone derivative was found to be an effective inhibitor for carbon steel corrosion in 1M HCl solution.
- Protection efficiency decreases with an increased temperature; the optimum concentration of PQPS for inhibition is 5ppm, indicates a physisorption inhibition process.
- The potentiodynamic polarisation measurements showed that PQPS inhibitor can be classified as a mixed complex inhibitor type (comprehensive adsorption) for inhibiting carbon steel in 1M HCl.
- The adsorption of the compound PQPS on carbon steel surface follows the Langmuir adsorption isotherm model.
- The negative value of $\Delta H_{ads.}$ means that the dissolution process is an exothermic phenomenon
- The activation enthalpy ΔH^* increase in the presence of the inhibitor implies that the PQPS increase the

height of the energy barrier of the corrosion process, and the positive sign of enthalpies ΔH^* reflects the endothermic nature of dissolution process.

REFERENCES

Abboud,Y., Abourriche, A., Saffaj, T., Berrada, M. and Charrouf, M. (2009) A. Bennamara, and H. Hannache, A novel azo dye, 8-quinolinol-5-azoantipyrine as corrosion inhibitor for mild steel in acidic media. Desalination, 237(1-3), 175-189.

Abd El-Lateef, H.M., Abbasov, V.M., Aliyeva, L.I., Qasimov, E.E. and Ismayilov, I.T. (2013) Inhibition of carbon steel corrosion in CO_2-saturated brine using some newly surfactants based on palm oil: experimental and theoretical investigations. Mater Chem. and Phys., 142(2-3), 502–512.

Ahmed, S. (2012) Synthesis and characterization of new heterocyclic derivati- ves containing cyclic imides. Ph.D. Thesis, Chem.Dept. College of Sci., Baghdad Univ.

Alafeefy, A.M. (2011) Some new quinazolin-4(3H)-one derivative, synthesis and antitumorm activity, J. Saudi Chem. Soc., 15(4), 337-343.

Al-Majidi, S.M.H. (2013) Synthesis, Characterization and Evaluation of Antimicrobial Activity of Several New N-Substituted Carbazole. J. Al-Nahrain Un.,16(4), 67-79.

Al-Majidi, S.M.H., ahmad, M.R. and Khan, A.K. (2013) Synthesis and characterization of novel 1,8-Naphthalimide derivatives containing 1,3-oxazoles, 1,3-thiazoles, 1,2,4-triazoles as antimicrobial agents. J.Al-Nahrain University, 16(4), 55-66.

Al-Majidi, S.M.H. and Al-Kaisy, W.N. (2009) Synthesis and Some Biological studies of new diazine, triazine, diazole, thiazole and 4-Oxazoline derivatives. Proceeding of 3rd scientific conference of the collage science, University of Baghdad. 1413-1423.

Almeida, C.M.V.B., Raboczkay, T. and Giannetti, B.F. (1999) Inhibiting effect of citric acid on the pitting corrosion of tin. Journal of applied electrochemistry, 29(1), 123-128.

Bahrami, M.J., Hosseini, S.M.A, Pilvar, P. (2010) Experimental and theoretical investigation of organic compounds as inhibitors for mild steel corrosion in sulfuric acid medium. Corros. Sci., 52(9), 2793–2803.

Becke, A.D. (1993) Density-functional thermochemistry. III, The role of exact exchange. J. Chem. Phys., 98(7), 5648-5652.

Behpour, M., Ghoreishi, S.M., Mohammadi, N., Soltani, N. and Salavati-Niasari, M. (2010) Investigation of some Schiff base compounds containing disulfide bond as HCl corrosion inhibitors for mild steel. Corros. Sci., 52(12), 4046–4057.

Bentiss, F., Lebrini, M. and Lagrenée, M. (2005) Thermodynamic characterization of metal dissolution and inhibitor adsorption processes in mild steel/2, 5-bis (n-thienyl)-1,3,4-thiadiazoles/hydrochloric acid system. Corrosion Science, 47(12), 2915-2931.

Bentiss, F., Traisnel, M. and Lagrenee, M. (2000) The substituted 1,3,4-oxadiazoles: a new class of corrosion inhibitors of mild steel in acidic media. Corros. Sci., 42(1), 127-146.

Chen, K., Wang, K., Kirichian, A.M. and Kassis, A.I. (2006) In silico design, synthesis, and biological evaluation of radioiodinated quinazolinone derivatives for alkaline phosphatase mediated cancer diagnosis and therapy. Mol. Cancer Ther., 5(12), 3001-3013.

Chermette, H. (1999) Chemical Reactivity Indexes in Density Functional Theory. J. Comput. Chem., 20(1), 129-154.

Dahmani, M., Et-Touhami, A., Al-Deyab, S.S., Hammouti, B. and Bouyanzer, A. (2010) Corrosion Inhibition of C38 Steel in 1M HCl: A Comparative Study of Black Pepper Extract and Its Isolated Piperine. Int. J. Electrochem. Sci., 5(8), 1060-1069.

Ebenso, E.E., Isabirye, D.A. and Eddy, N.O. (2010) Adsorption and quantum chemical studies on the inhibition potentials of some thiosemicarbazides for the corrosion of mild steel in acidic medium. Int. j. mol. sci., 11(6), 2473-2498.

Fontana, M.G. (1987) Corrosion Engineering. 3rd Ed., McGraw-Hill Book Company, New York, 346.

Frisch, M.J., Trucks, G.W., Schlegel, H.B., Scuseria, G.E., Robb, M.A., Cheeseman, J.R., Montgomery, J.A., Jr., Vreven, T., Kudin, K.N., Burant, J.C., Millam, J.M., Iyengar, S.S., Tomasi, J., Barone, V., Mennucci, B., Cossi, M., Scalmani, G., Rega, N., Petersson, G.A., Nakatsuji, H., Hada, M., Ehara, M., Toyota, K., Fukuda, R,. Hasegawa, J., Ishida, M., Nakajima, T., Honda, Y., Kitao, O., Nakai, H., Klene, M., Li, X., Knox, J.E., Hratchian, H.P. Cross, J.B. Bakken, V. Adamo, C. Jaramillo, J., Gomperts, R., Stratmann, R.E., Yazyev, O., Austin, A.J., Cammi, R., Pomelli, C., Ochterski, J.W., Ayala, P.Y., Morokuma, K.,Voth, G.A., Salvador, P., Dannenberg, J.J., Zakrzewski, V.G., Dapp: rich, S., Daniels, A.D., Strain, M.C., Farkas, O., Malick, D.K., Rabuck, A.D., Raghavachari, K., Foresman, J.B., Ortiz, J.V., Cui, Q., Baboul, A.G., Clifford, S., Cioslowski, J., Stefanov, B.B., Liu, G., Liashenko, A., Piskorz, P., Komaromi, I., Martin, R.L., Fox, D.J., Keith, T., Al-Laham, M.A., Peng, C.Y., Nanayakkara, A., Challacombe, M., Gill, P.M.W., Johnson, B., Chen, W., Wong, M.W., Gonzalez, C. and Pople, J.A. **(2009)** Gaussian 09. Revision E.01, Gaussian, Inc. Wallingford CT.

Gad, A.G. and Tamous, H.M. (1990) Structural investigation of pyrazole derivatives as corrosion inhibitors for delta steel in acid chloride solutions, Journal of Applied Electrochemistry, 20(3), 488-493.

Geerlings, P. and Proft, F.D. (2002) Chemical Reactivity as Described by Quantum Chemical Methods. International Journal of Molecular Sciences, 3(4), 276-309.

Gomma, G.K. and Wahdan, M.H. (1995) Schiff bases as corrosion inhibitors for aluminium in hydrochloric acid solution. Materials chemistry and physics, 39(3), 209-213.

Joule, J. and Mills, K. (2010) Heterocyclic Chemistry. 5th ed., John Wiley & Sons, Inc. USA.

Kandemirli, F. and Sagdinc, s. (2007) Theoretical study of corrosion inhibition of amides and thiosemicarbazones. Corrosion Science, 49(5), 2118–2130.

Khaled, K.F. (2008) Adsorption and inhibitive properties of a new synthesized guanidine derivative on corrosion of copper in 0.5 M H_2SO_4. Appl. Surf. Sci., 255(5), 1811-1818.

Khaled, K.F. (2008) Application of electrochemical frequency modulation for monitoring corrosion and corrosion inhibition of iron by some indole derivatives in molar hydrochloric acid. Mater. Chem. Phys., 112(1), 290–300.

Lee, C, Yang, W. and Parr, R.G. (1988) Development of the Colle-Salvetti correlation energy formula into a functional of the electron density. Phys. Rev., B 37(2), 785-789.

Li, X., Deng, S. and Fu, H. (2012) Allyl thiourea as a corrosion inhibitor for cold rolled steel in H_3PO_4 solution. Corros. Sci., 55, 280–288.

Limousin, G., Gaudet, J.P., Charlet, L., Szenknect, S., Barthes, V. and Krimissa, M. (2007) Sorption isotherms: a review on physical bases, modeling and measurement. Appl Geochem, 22(2), 249–275.

Lukovits, I., Kalman, E. and Zucchi, F. (2001) Corrosion inhibitors—correlation between electronic structure and efficiency. Corrosion, 57(1), 3-8.

Maayta, A.K. and Al-Rawashdeh, N.A.F (2004) Inhibition of acidic corrosion of pure aluminum by some organic compounds. Corros. Sci., 46(5), 1129-1140.

March, J. (1985) Advanced Organic Chemistry. 3rd ed.,Wiley, New York, USA.

Migahed, M.A. (2005) Electrochemical investigation of the corrosion behaviour of mild steel in 2M HCl solution in presence of 1-dodecyl-4-methoxy pyridinium bromide. Materials chemistry and physics, 93(1), 48-53.

Mora, N., Cano, E., Polo, J.L., Puente, J.M. and Bastidas, J.M. (2004) Corrosion protection properties of cerium layers formed on tinplate. Corrosion science, 46(3), 563-578.

Obot, I.B. and Obi-Egbedi, N.O (2008) Inhibitory effect and adsorption characteristics of 2, 3-diaminonaphthalene at aluminum/hydrochloric acid interface: experimental and theoretical study. 15(6), 903-910.

Obot, I.B. and Obi-Egbedi, N.O. (2010) Theoretical study of benzimidazole and its derivatives and their potential activity as corrosion inhibitors. Corros. Sci., 52(2), 657-660.

Parr, R.G. and Yang, W. (1989) Density Functional Theory of Atoms and Molecules. 1ST Edn., Oxford University Press: New York.

Poorqasemi, E., Abootalebi, O., Peikari, M., Haqdar, F. (2009) Investigating accuracy of the Tafel extrapolation method in HCl solutions. Corros. Sci., 51(5), 1043– 1054.

Raja, P.B. and Sethuraman, M.G. (2008) Atropine sulphate as corrosion inhibitor for mild steel in sulphuric acid medium. Mater. Lett., 62(10-11), 1602–1604.

Rani, B.E.A. and Basu, B.B.J. (2012) Green Inhibitors for Corrosion Protection of Metals and Alloys: An Overview. International Journal of Corrosion, 1, 1-15.

Riggs Jr, O.L. and Hurd, R.M (1967) Temperature coefficient of corrosion inhibition. Corrosion, 23(8), 252-260.

Safak, S., Duran, B.,Yurt, A., and Turkog˘lu, G. (2012) Schiff bases as corrosion inhibitor for aluminium in HCl solution. Corros. Sci., 54, 251–259.

Saxena, N., Kumar, S. and Mathur, S.P. (2009) Anisalidine derivatives as corrosion inhibitors of mild steel in acidic media. 1. Chem. Eng. Commun., 196(12), 1451–1465.

Shetty, S.D., Shetty, P. and Nayak, H.V.S (2007) The inhibition action of N-(furfuryl)-N- phenyl thiourea on the corrosion of mild steel in hydrochloric acid medium. Mater. Lett. 61(11), 2347–2349.

Shriner, R., Fuson, R., Cartin, D. and Morril, T. (1980) The systematic Identification of Organic Compounds. 8th ed., John Wiley and Sons, New York, USA.

Singh, A.K. and Quraishi M.A. (2012) Study of some bidentate Schiff bases of isatin as corrosion inhibitors for mild steel in hydrochloric acid solution. Int. J. Electrochem. Sci., 7(4), 3222–3241.

Singh, A., Singh, V.K. and Quraishi, M.A. (2010) Effect of fruit extracts of some environmentally benign green corrosion inhibitors on corrosion of mild steel in hydrochloric acid solution. J. Mater. Environ. Sci., 1(3), 162-174.

Trabanelli, G. and Mansfeld, F. (Ed) (1987) Corrosion mechanism. Mercel Dekker, New York, 119.

Wang, H., Wang, X., Wang, H., Wang, L. and Liu, A. (2007) DFT study of new bipyrazole derivatives and their potential activity as corrosion inhibitors. Journal of Molecular Modeling, 13(1), 147-153.

Zarrouk, A., Dafali, A., Hammouti, B., Zarrok, H., Boukhris, S. and Zertoubi, M. (2010) Synthesis, characterization and comparative study of functionalized quinoxaline derivatives towards corrosion of copper in nitric acid medium. Int. J. Electrochem. Sci., 5, 46-55.

Zhang, J., Liu, J., Yu, W., Yan, Y., You, L. and Liu, L. (2010) Molecular modeling of the inhibition mechanism of 1-(2-aminoethyl)-2-alkyl-imidazoline. Corrosion Science, 52(6), 2059-2065.